RMetS

Royal Meteorological Society

The precipitation response to the desiccation of Lake Chad

D. Lauwaet,[a,b]* N. P. M. van Lipzig,[a] K. Van Weverberg,[a,c] K. De Ridder[b] and C. Goyens[a,d]

[a]*Department of Earth and Environmental Sciences, Katholieke Universiteit Leuven, Heverlee, Belgium*
[b]*Vlaamse Instelling voor Technologisch Onderzoek (VITO), Mol, Belgium*
[c]*Atmospheric Sciences Division, Brookhaven National Laboratory, Upton, NY, USA*
[d]*Univ Lille Nord de France, ULCO, LOG, F-62930 Wimereux, France, CNRS, UMR 8187, F-62930 Wimereux, France*

Correspondence to: D. Lauwaet, Department of Earth and Environmental Sciences, Katholieke Universiteit Leuven, Celestijnenlaan 200E, Heverlee 3001, Belgium. E-mail: dirk.lauwaet@ees.kuleuven.be

Located in the semi-arid African Sahel, Lake Chad has shrunk from a surface area of $25\,000\,km^2$ in 1960 to about $1350\,km^2$ due to a series of droughts and anthropogenic influences. The disappearance of such a large open-water body can be expected to have a noticeable effect on the meteorology in the surroundings of the lake. The impact could extend even further to the west as westward propagating convective systems pass Lake Chad in the rainfall season. This study examines the sensitivity of the regional hydrology and convective processes to the desiccation of the lake using a regional atmospheric model. Three Lake Chad scenarios are applied reflecting the situation in 1960, the current situation and a potential future scenario in which the lake and the surrounding wetlands have disappeared. The model simulations span the months July–September in 2006, which includes the rainfall season in the Lake Chad area. Total precipitation amounts and the components of the hydrological cycle are found to be hardly affected by the existence of the lake. A filled Lake Chad does, however, increase the precipitation at the east side of the lake. The model results indicate that the boundary layer moisture and temperature are significantly altered downwind of the lake. By investigating a mesoscale convective system (MCS) case, this is found to affect the development and progress of the system. At first, the MCS is intensified by the more unstable boundary layer air but the persistence of the system is altered as the cold pool propagation becomes less effective. The proposed mechanism is able to explain the differences in the rainfall patterns nearby Lake Chad between the scenarios. This highlights the local sensitivity to the desiccation of Lake Chad whereas the large-scale atmospheric processes are not affected. Copyright © 2011 Royal Meteorological Society

1. Introduction

Lake Chad was once one of the largest lakes in Africa, with a surface area of about $25\,000\,km^2$. However, because of a series of droughts that began in the 1960s, the lake has shrunk to almost one-twentieth of its maximum area: $1350\,km^2$. The only remaining area of permanent open water is located in the southern region of the lake basin, where it is surrounded by densely vegetated swamps and smaller pools. Not only climate, but also anthropogenic influences like the drilling of boreholes and large-scale irrigation systems have played their role in the demise of the lake (Birkett, 2000).
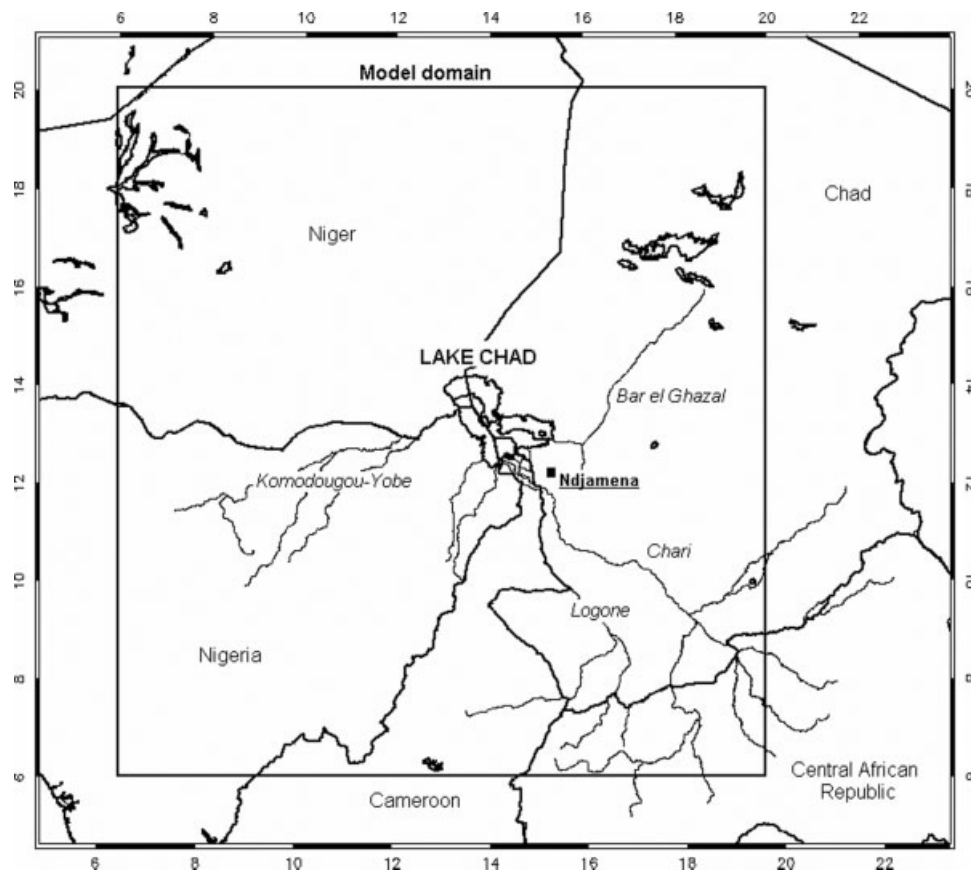
Figure 1. Situation map of the study area.

Both led to high evaporation losses of water that would normally reach the lake. Changes in the regional rainfall patterns combined with human impact have thus led to the slow desiccation of Lake Chad from the north to the south.

The geographical situation of Lake Chad is shown in Figure 1. The Lake Chad basin is very flat and the lake is shallow, with a maximum depth around 7 m. The source of the lake's water is run-off from the mountains far to the south, in the humid uplands of Cameroon and the Central African Republic. The Chari and Logone rivers alone account for 80% of the lake's annual inflow, which is around 40 km^3 (Hutchinson *et al.*, 1992). Most of the agricultural activities in the Lake Chad region occur along these two rivers. The lake is a closed basin without outflow and loses its water mainly through evaporation, with annual rates as large as 3000 mm.

The objective of this study is to look in detail at how passing mesoscale convective systems (MCS) and associated rainfall of these systems are affected by the presence of Lake Chad. This information is useful for understanding the effect of the desiccation of Lake Chad in the semi-arid Sahel environment on the local meteorological conditions. The impact could extend even further to the west as a lot of westward propagating convective systems pass the lake in the rainfall season. This hypothesis is tested in this study by using a regional atmospheric model. The term MCS in this study is used for westward propagating organized clusters of deep convection that merge into one single mesoscale cloud shield. These systems are found to produce 80–90% of the annual rainfall in the Sahel area (Mathon *et al.*, 2002).

The model used in this paper is the Advanced Regional Prediction System (ARPS), a mesoscale atmospheric model developed at the University of Oklahoma (Xue *et al.*, 2000, 2001). To account for the interaction with the soil and vegetation, a Soil–Vegetation–Atmosphere Transfer (SVAT) model developed by De Ridder and Schayes (1997) and adapted for the Sahelian environment is coupled to ARPS. The coupled model is previously evaluated and used in different modelling studies in the Sahel region (Lauwaet *et al.*, 2008). To assess the impact of the shrinking of Lake Chad, a scenario analysis is applied. First, the rainfall season of 2006 (July–September) with the current Lake Chad situation is simulated by the model and the results are validated. Afterwards, simulations are performed with completely filled Lake Chad scenarios and a scenario in which the lake and the surrounding wetlands have disappeared.

The possible impacts of increases in inland water storages and irrigation on the atmosphere have already been studied in different parts of the world. Bonan (1995) tested the sensitivity of simulations with a general circulation model to the inclusion of inland water surfaces. For Africa, precipitation amounts did not change except for the Great Lakes region. In the USA, Segal *et al.* (1998) used a mesoscale model to investigate the rainfall response to irrigation. They found that irrigation did indeed alter existing rainfall regions but no new rainfall areas were generated. Hope *et al.* (2004) examined the meteorological response to permanent inland water in an arid region of Australia. The large-scale interaction between the atmosphere and the land surface was not affected by the existence of the inland water. Away from the imposed water expanse, no consistent response in rainfall was found. And in Sudan, the impact of draining a large wetland in the Nile basin on the regional
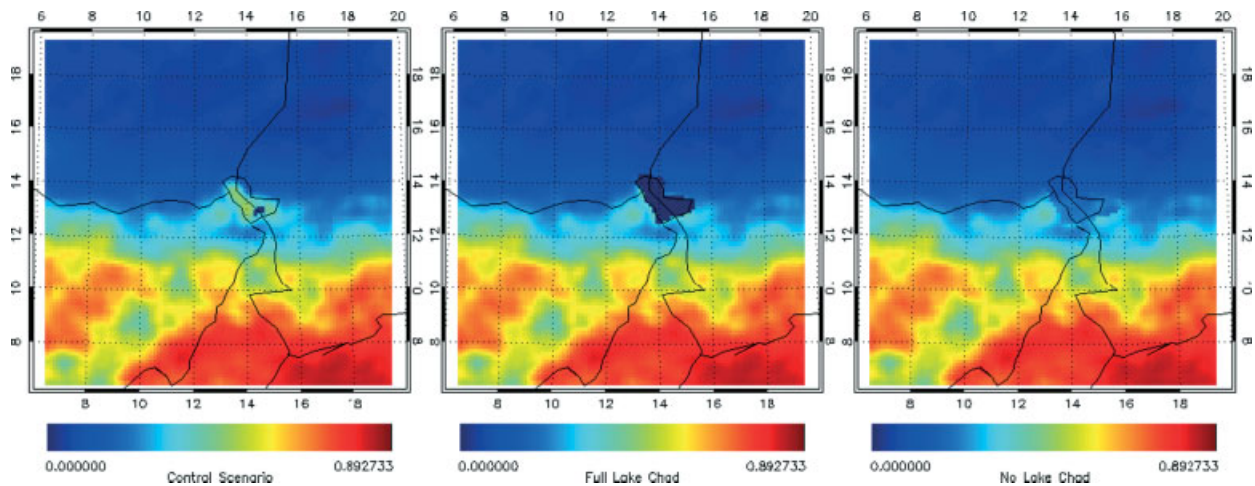
Figure 2. Vegetation cover values in July 2006 for the three scenarios.

water cycle was found to be negligible in regional model simulations (Mohamed *et al.*, 2005).

Although the impact on the precipitation is small in each of the cases mentioned above, all studies report significant changes in local temperatures and evaporation rates. As the land surface in the Sahel is known to play an important role in the initiation and development of convective systems (Mohr *et al.*, 2003; Taylor *et al.*, 2010), such changes may well have an impact on the convective activity in the region of Lake Chad. Lauwaet *et al.* (2009) showed that even a 20% vegetation change can have a significant effect on precipitation amounts from an MCS in West Africa.

In this paper we first outline the characteristics of both the regional atmospheric model and the SVAT model in section 2. The results of the coupled model for the 2006 rainy season are evaluated in section 3. Afterwards the two Lake Chad scenarios are applied and the results are presented and discussed in section 4. Conclusions are given in section 5.

2. Numerical model and experiment design

2.1. Atmospheric model

The model used for this study is the Advanced Regional Prediction System (ARPS), a non-hydrostatic mesoscale atmospheric model developed at the University of Oklahoma (Xue *et al.*, 2000, 2001). It includes conservation equations for momentum, heat, mass, water (vapour, liquid and ice), sub-grid scale turbulent kinetic energy and the state equation of moist air. The model contains detailed parametrizations for cloud microphysics, cumulus convection and radiation transfers. In our model set-up, the 1.5-order Turbulent Kinetic Energy (TKE) model is used to represent turbulence. The parametrization scheme of Schultz (1995) accounts for the model microphysics, while the Kain–Fritsch cumulus parameterization scheme solves the cumulus convection (Kain and Fritsch, 1990).

Data with a 0.25° horizontal resolution from the global operational analysis by the European Centre for Medium-Range Weather Forecasts (ECMWF) are used as initial conditions and as 6-hourly lateral boundary conditions for the model runs. The ECMWF AMMA reanalysis data, a special dataset for this period in which a radiosonde humidity bias was corrected over West Africa, have not been used as these data showed no improvement of precipitation in the study domain and the horizontal resolution is coarser than in the operational analysis (Agusti-Panareda *et al.*, 2010). The ARPS model domain has a grid spacing of 15 km and a domain size of 1500 km × 1500 km, centred over the western shore of Lake Chad (13°E, 13°N) (Figure 1). In all simulations, 40 vertical levels are employed with a grid spacing of 25 m near the surface, increasing to 1 km near the upper model boundary, located at 25 km altitude. The simulations are initialized on 1 July 2006 at 0000 LT and run until 30 September 2009 at 2400 LT. Tests were performed to quantify the impact of a spin-up period of 1 month, with the model being initialized on 1 June 2006. The model results proved to be rather insensitive to the spin-up time, the domain-wide precipitation decreased slightly (less than 5%) in the case of a longer spin-up.

2.2. Land surface model

The land surface model coupled to ARPS is a one-dimensional SVAT model, developed by De Ridder and Schayes (1997). The model consists of one vegetation layer and six soil layers; energy and water budgets are calculated separately for both the soil and the vegetation and weighted by their respective cover fractions. Soil heat and water transfer equations are numerically solved using the Crank–Nicholson iteration technique. Canopy temperature and moisture content (both inside and on the leaves) are solved with prognostic equations. A particular feature of the model is the use of a physically based parametrization of the transpiration process, requiring only one empirical function in the stomatal resistance formulation. The model is adjusted to deal with the soil and vegetation conditions in the Sahel (Lauwaet *et al.*, 2008). To take into account the effect of a soil crust, which is present in most parts of the Sahel area, the saturated hydraulic conductivity is lowered by one order of magnitude, following Vandervaere *et al.* (1997). Other specifications concerning the model set-up can be found in Lauwaet *et al.* (2009).

As the vegetation in the Sahel is known to grow and decline during the course of a rainy season, vegetation cover and leaf area index (LAI) values are made time dependent. Details of the vegetation cover and LAI calculations can be found in the Appendix. Note that an assumption of natural vegetation cover is made everywhere in the model domain.

As there are some agricultural areas present in the study area, especially to the south of Lake Chad, this assumption might have an impact on the surface fluxes and consequently on the sensitivity of the model to the presence of the lake.

Measured values of soil temperature and soil moisture are scarce in this region; therefore initial values for the land surface model are taken from measurements of the HAPEX-Sahel database, where typical values for this period of the year in the Sahel can be found. The uniform initialization is a simplification of the real situation, although the effects are limited in time as the sandy topsoil dries out in a few days and convective systems bring rain to the southern part of the study area already in the first days of the simulation. Initial water temperatures for Lake Chad are obtained from measurements of the International Lake Environment Committee during the period 1956–1960 (www.ilec.or.jp). The temperature of the lake is held constant at 304 K, the average lake temperature in the period July–September.

2.3. Sensitivity experiments

To investigate whether the desiccation of Lake Chad has a significant influence on the regional meteorology and precipitation amounts, sensitivity experiments are carried out. In the control scenario, Lake Chad covers an area of 1350 km^2 and is surrounded by densely vegetated marshlands (Figure 2). This corresponds to the permanent lake area, reported by Birkett (2000). The marshlands are taken into account in the model by providing them with continuously high soil moisture values (80% saturation) below a depth of 0.25 m. To represent the situation in 1960, when the lake surface spanned 25 000 km^2, a second scenario is applied. Furthermore, it is interesting to know what the impact would be if Lake Chad and the surrounding wetlands were to completely disappear. Therefore, a third scenario is applied in which the lake and the dense vegetation in the lake basin are replaced by average vegetation cover values for these latitudes.

To quantify the impact of different Lake Chad temperatures on the results that are presented in section 4.4, two more scenario simulations with a large Lake Chad surface are performed, applying the minimum (300 K) and maximum (308 K) temperature values that are reported in the International Lake Environment Committee database.

3. Comparison with observations

In order to evaluate the modelled rainfall results in the study area, monthly composite rainfall images from the Tropical Rainfall Measurement Mission (TRMM) satellite are used, which are corrected with data from rainfall stations in the region. A comparison with the simulated rainfall amounts in the control scenario for the total modelled period (July–September 2006) is made in Figure 3. The overall pattern of the rainfall is well reproduced, with the highest rainfall amounts in the mountainous regions in the south of the study domain and gradually decreasing amounts to the north. In both the observations and the model, there is a local minimum above and to the west of Lake Chad. However, the precipitation is clearly underestimated by the model, with an overall underestimation in the study domain of 30%. This underestimation is due to the ECMWF boundary data, which are known to underestimate the rainfall in the northern Sahel areas (Andersson *et al.*, 2005; Agusti-Panareda *et al.*, 2009).
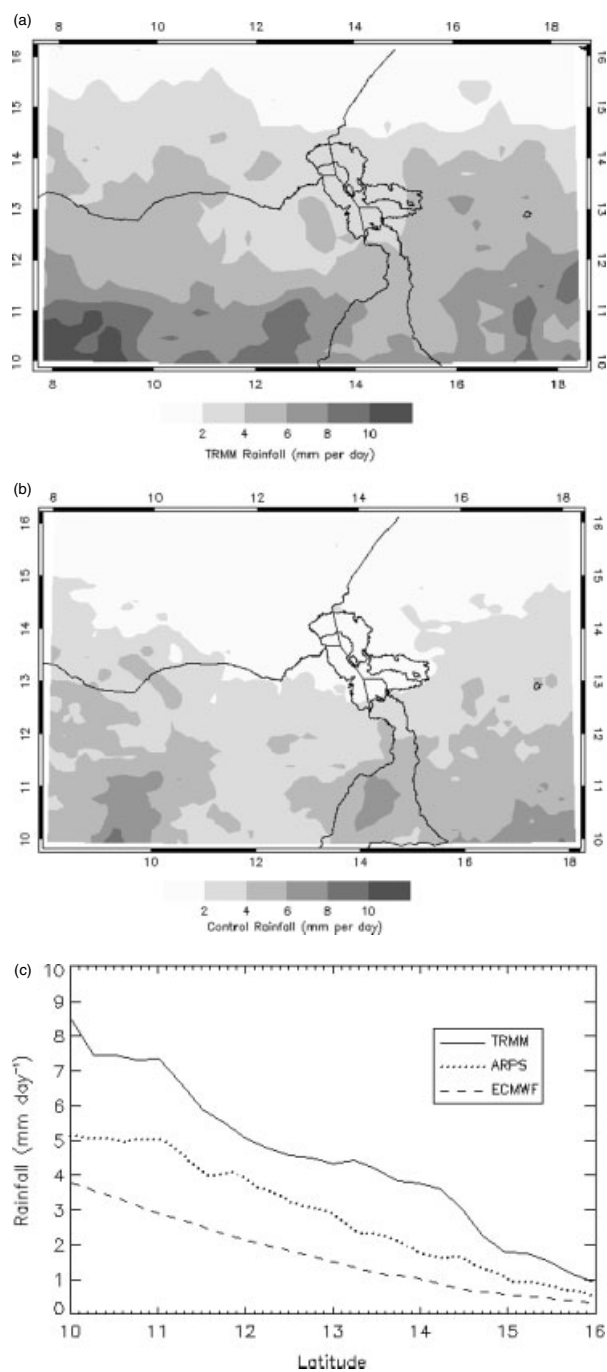
Figure 3. Comparison between the observed rainfall amounts for the entire simulated period from the TRMM satellite (a), the modelled rainfall amounts (b) and the rainfall gradient, averaged per latitude band (c).

This is demonstrated in Figure 3(c), which shows the rainfall gradient in the study area. The ARPS model shows a clear improvement over the rainfall amounts from the ECMWF boundary data. Given this fact, the model does a reasonably good job in reproducing the overall structure of the rainfall in the Lake Chad region. It is considered that the control rainfall is sufficiently similar to the observations to render the different Lake Chad experiments interesting.

A further comparison between the ARPS model and the ECMWF data is given in Figure 4. Overall, the differences, averaged over the entire simulated period, are small, with air temperature differences less than 1 K and specific humidity differences less than 1 g kg^{-1}. The largest changes occur close to the surface, in the planetary boundary layer, which

Figure 5. Series of meteorological parameters modelled at the ground surface (location 14°E, 13°N) during the passage of the MCS of 17 July 2006 in the No LC scenario.
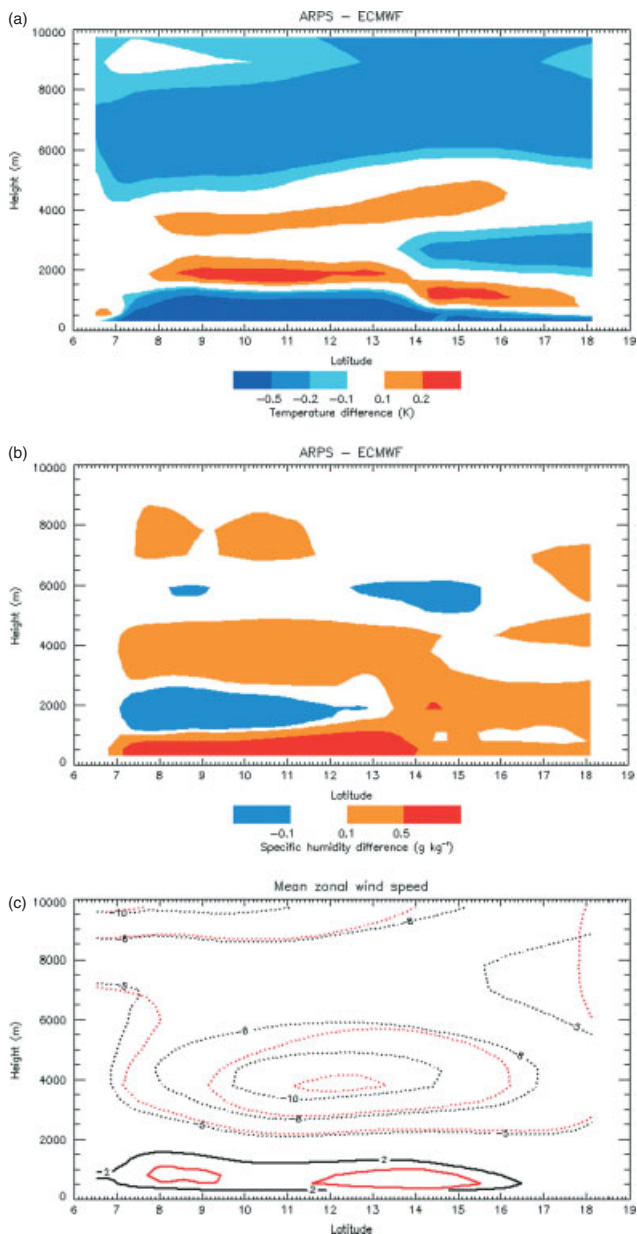

Figure 4. (a) Temperature difference, averaged per latitude band, between the ARPS model and the ECMWF analysis data for the entire simulated period. (b) Specific humidity difference, averaged per latitude band, between the ARPS model and the ECMWF analysis data for the entire simulated period. (c) Mean zonal wind speed, averaged per latitude band, in the ARPS model (black) and ECMWF analysis data (red) for the entire simulated period.

is slightly cooler and moister in the ARPS model due to larger evaporation amounts in comparison to the ECMWF model. Although the changes are small, they have a significant effect on the average convective available potential energy (CAPE) values, a measure which is closely linked to convective intensity in the Sahel (Taylor *et al.*, 1997; Clark *et al.*, 2004). Concerning the wind speeds, the westerly flow above the surface is slightly increased in the ARPS model, as is the African easterly jet (AEJ), which can be noticed around 400 hPa. This will result in higher amounts of shear in the ARPS model, and consequently more potential to initiate convection. Both the increase in CAPE and shear can explain the higher rainfall amounts in the ARPS model in comparison to the ECMWF model.
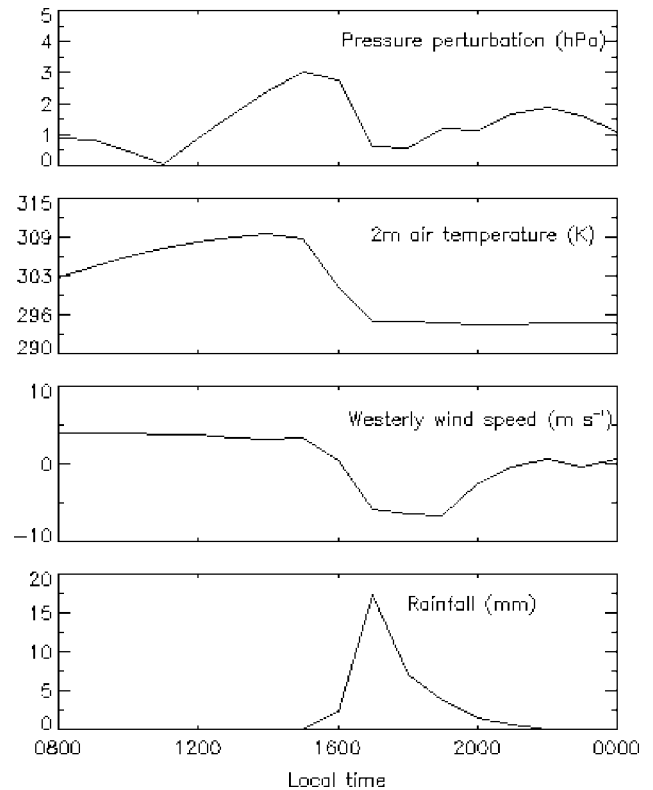
In this paper, much attention is given to the large-scale organized storm systems that pass through the study area – the mesoscale convective systems. It is thus important that the ARPS model can realistically produce such systems. Figure 5 shows a series of meteorological parameters that are modelled during the passing of an MCS on 17 July 2006, which will be further studied in section 4.4. These parameters show the typical behaviour of the passage of an MCS, with a pressure increase when the system approaches, a sudden drop of temperature when the system arrives around 1500 LT and a sudden change in wind direction and intensity at the same time. The convective core of the system produces a peak rainfall rate, followed by a period of light rain when the stratiform region of the MCS passes. These model results are in good agreement with observations made during the passage of an MCS (Chong *et al.*, 1987).

In order to evaluate the vertical structure of the modelled MCS, a comparison can be made with hydrometeor profiles from the TRMM microwave imager, a five-channel microwave radiometer which measures cloud liquid and ice water, rainfall, snow and hail (Figure 6). To make a correct comparison, the modelled hydrometeor profiles are interpolated to the same horizontal (0.5°) and vertical (500 m to 4 km) resolution as the measured ones. Unfortunately, the timing of the system differs between model and reality as the satellite observed the MCS of 17 July 2006 at 0300 LT whereas the system only developed in the model in the late afternoon. Clearly, the modelled convection is deeper and the system is smaller than observed in reality. This may be due to the timing difference, as there is more convective energy available in the late afternoon. However, the amount of hydrometeors in the MCS corresponds well between model and observations, with the highest amounts
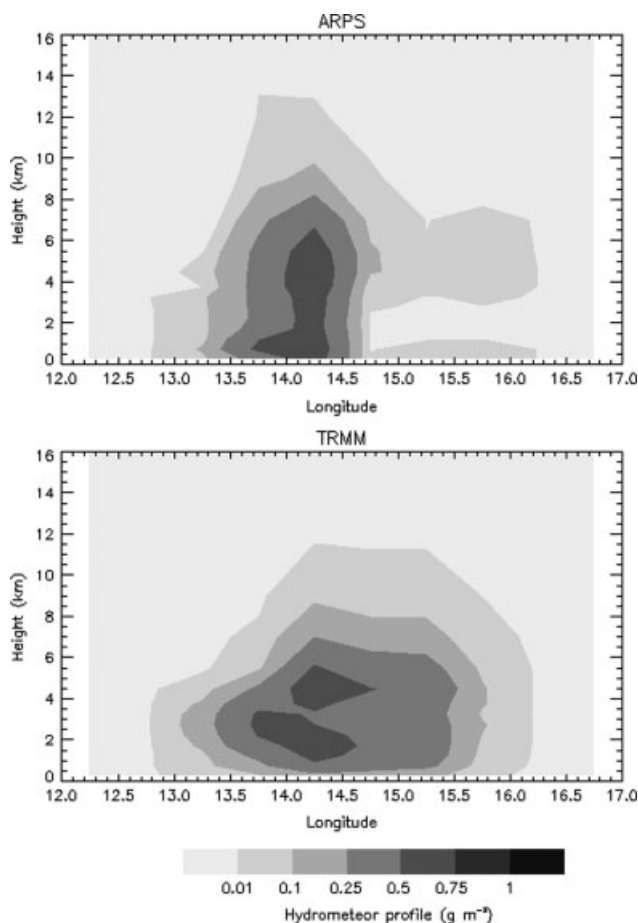
Figure 6. Upper panel: modelled hydrometeor profile at 13°N at 1800 LT of the MCS case on 17 July 2006 in the No LC scenario. Lower panel: observed hydrometeor profile from the TRMM microwave imager at 12°N at 0300 LT.

around 1 g m^{-3} and decreasing amounts going into the trailing stratiform region.

To investigate the impact of Lake Chad on passing MCS, as will be done in section 4.4, it is important to evaluate the amount of MCS produced by the model in this region. Therefore, a mesoscale convective system counting procedure is used, based on a method comparable to Taylor and Clark (2001) and applied in Lauwaet *et al.* (2009). An MCS is identified whenever the westerly wind component at the ground surface deviates from its 24 h running mean by at least 4 m s^{-1}. This is a typical feature of a passing MCS, as can be seen in Figure 5. Events have to be spaced in time for at least 12 h. The procedure is applied on the results of the simulation without Lake Chad, as in this case there is no interference with the lake.

A different method is used to assess the observed number of MCS, based on hourly Meteosat-8 infrared (10.8 μm) images. MCS are identified assuming that strong convective activity is related to low brightness temperatures, using an algorithm developed by Schröder *et al.* (2009) and applied over the Lake Chad region by Goyens *et al.* (2011). A single system is defined as a contiguous area of pixels with a brightness temperature below 233 K exceeding 30 000 km^2. This definition results from a visual inspection of the systems on the Meteosat images and is close to the definition given by Laurent *et al.* (1998). The results from both the model and the observations are presented in Figure 7. Although the methods are completely different and one must be careful

drawing strong conclusions, the results indicate that the model is able to approach the number of MCS that can be observed in reality passing over Lake Chad. The timing of the events differs between model and observations, with more events in August in the model, and fewer in September.

4. Impact of Lake Chad

4.1. Rainfall pattern

To assess the impact of the desiccation of Lake Chad on the regional precipitation pattern, the model is run with three different Lake Chad scenarios. Simulations are performed with a completely filled Lake Chad with a 25 000 km^2 surface (Full LC), the current situation in which the lake occupies 1350 km^2, surrounded by wetlands (Control), and a possible future scenario in which the lake is replaced by normal vegetation (No LC). Differences in rainfall amounts for the total simulated period are presented in Figure 8. Compared to the control run, there is a clear increase in precipitation over the lake and its eastern border when the lake is filled. Total rainfall amounts more than double in this region. In the other parts of the study area, some small changes can be observed, but no clear trend is visible. Overall, there is only a slight increase in total precipitation over the model domain (Table I).

The second panel of Figure 8 shows the comparison between the model run in which Lake Chad has disappeared and the control run. The complete desiccation of the lake clearly has a minor influence on the precipitation as only small changes are visible, probably due to a slightly different track of some intense precipitating systems. Also, the total rainfall amounts hardly change. When the situations with a completely filled and without Lake Chad are compared, the same pattern as in the upper panel appears. The precipitation is clearly increased over the eastern side of the lake, and a slight decrease over the western border becomes visible. Over the study domain as a whole, there are only minor alterations of the total rainfall amounts for the 2006 rainfall season.

These results compare well to previous model experiments with water bodies in semi-arid areas. In model experiments in which Lake Eyre in inland Australia was filled, the rainfall response was also limited to the lake and its borders (Hope *et al.*, 2004). Given a large enough lake, a precipitation response was found, but the response away from the lake was unclear and variable. Segal *et al.* (1998) investigated the impact of irrigation on rainfall in the USA with a mesoscale model and found only weak alterations of the rainfall fields. And in Sudan, the effect of draining a large wetland in the Nile basin was found to be insignificant relative to the inter-annual variability of the precipitation (Mohamed *et al.*, 2005). Our results thus confirm that creating a large water body in a semi-arid environment is unlikely to produce a widespread precipitation increase.

4.2. Microclimate

Although the changes in precipitation between the different scenarios are relatively small, there are significant changes in some local meteorological variables. To assess the effect of the changed land surface on the atmosphere, the mean diurnal cycle of sensible and latent heat fluxes over the Lake Chad area is presented in Figure 9(a). The differences
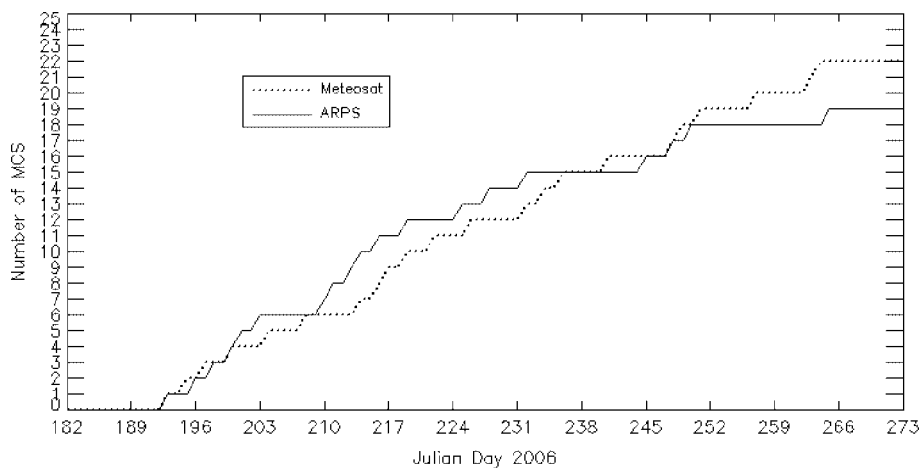
Figure 7. Comparison between the observed number of MCS, passing over Lake Chad (14°E, 12−15°N), during the entire simulated period from Meteosat images and the simulated number of MCS in the NoLC scenario.

Table I. Components of the water balance over the total study area and the region where most precipitation changes occur.

	Control		Full LC		No LC	
	Absolute (kg)	Relative	Absolute (kg)	Relative	Absolute (kg)	Relative
8−18°E; 10−16°N						
Q_{in}	2.42×10^{15}	1134	2.42×10^{15}	1142	2.41×10^{15}	1135
Q_{out}	2.37×10^{15}	1107	2.38×10^{15}	1119	2.36×10^{15}	1107
E	1.64×10^{14}	77	1.84×10^{14}	86	1.61×10^{14}	75
Rain	2.14×10^{14}	100	2.24×10^{14}	105	2.12×10^{14}	99
dQ_{dom}	7.77×10^{12}	4	8.04×10^{12}	4	8.01×10^{12}	4
12−17°E; 12.5−15°N						
Q_{in}	1.16×10^{15}	4124	1.17×10^{15}	4143	1.16×10^{15}	4127
Q_{out}	1.16×10^{15}	4123	1.18×10^{15}	4176	1.16×10^{15}	4112
E	3.03×10^{13}	107	4.78×10^{13}	169	2.57×10^{13}	91
Rain	2.83×10^{13}	100	3.65×10^{13}	129	2.80×10^{13}	99
dQ_{dom}	1.96×10^{12}	6	2.04×10^{12}	7	2.00×10^{12}	7

Q_{in}, incoming atmospheric moisture; Q_{out}, outgoing atmospheric moisture; E, evaporation; Rain, rainfall; dQ_{dom}, change of atmospheric moisture inside the domain. In the column 'Relative', values are normalized by the rainfall in the Control scenario.

between the scenarios are large as the fluxes for the No LC scenario show a clear 'land-like' behaviour, while the fluxes in the Full LC scenario show a 'water-like' behaviour. A slight reduction of the latent heat fluxes in the late afternoon in the Full LC scenario can be noticed, which is due to the fact that the boundary layer becomes more saturated during the course of the day.

The impact of the fluxes on the overlying atmosphere is shown in Figure 9(b) and (c), in which vertical cross-sections are compared along 13.3°N and 14.5°E respectively, hence crossing Lake Chad, for the Full LC and No LC scenarios. The figures present the differences in 3-month mean values of air temperature, specific humidity and wind speeds. The perturbations in air temperature and specific humidity are dominated by the overall wind direction at the surface, consistently southwest, as they are located downwind of Lake Chad. The lake effect is clearly limited to the boundary layer. During the night, Lake Chad is warmer than its surroundings and warms the overlying air. The effect is limited to the lake area as there is almost no wind during the night. During daytime, on the other hand, the lake is colder than the environment and cools the overlying air, which is transported to the northeast by the southwesterly surface

winds. Downwind of Lake Chad, the air is not only colder, but also moister when Lake Chad is filled.

Concerning the wind speeds, the main effect is the increase in wind speeds over the lake, due to the smaller roughness length there. During daytime the atmospheric cooling over the lake results in a lower boundary layer which forces the background flow between 1.5 and 2 km height (from northeast to southwest) to a downward motion. It should be noted that the changes in wind speed and direction are small compared to their background values. As demonstrated in previous studies (e.g. Segal *et al.*, 1997; Weaver, 2004) it can be expected that a daytime lake breeze develops in the case of a full Lake Chad, forced by the heterogeneity of the surface fluxes close to and over the lake. Although the horizontal model resolution is rather coarse for this kind of feature, a small lake breeze effect to the east and south of the lake can be noticed during daytime in Figure 9(b) and (c). However, the effect is small and apparently played no role in the precipitation processes in our model simulations, as can be seen from the precipitation results (Figure 8).

In their model experiments, Mohamed *et al.* (2005) found similar effects on the microclimate when draining a large wetland in the Nile basin. The influence on temperature and
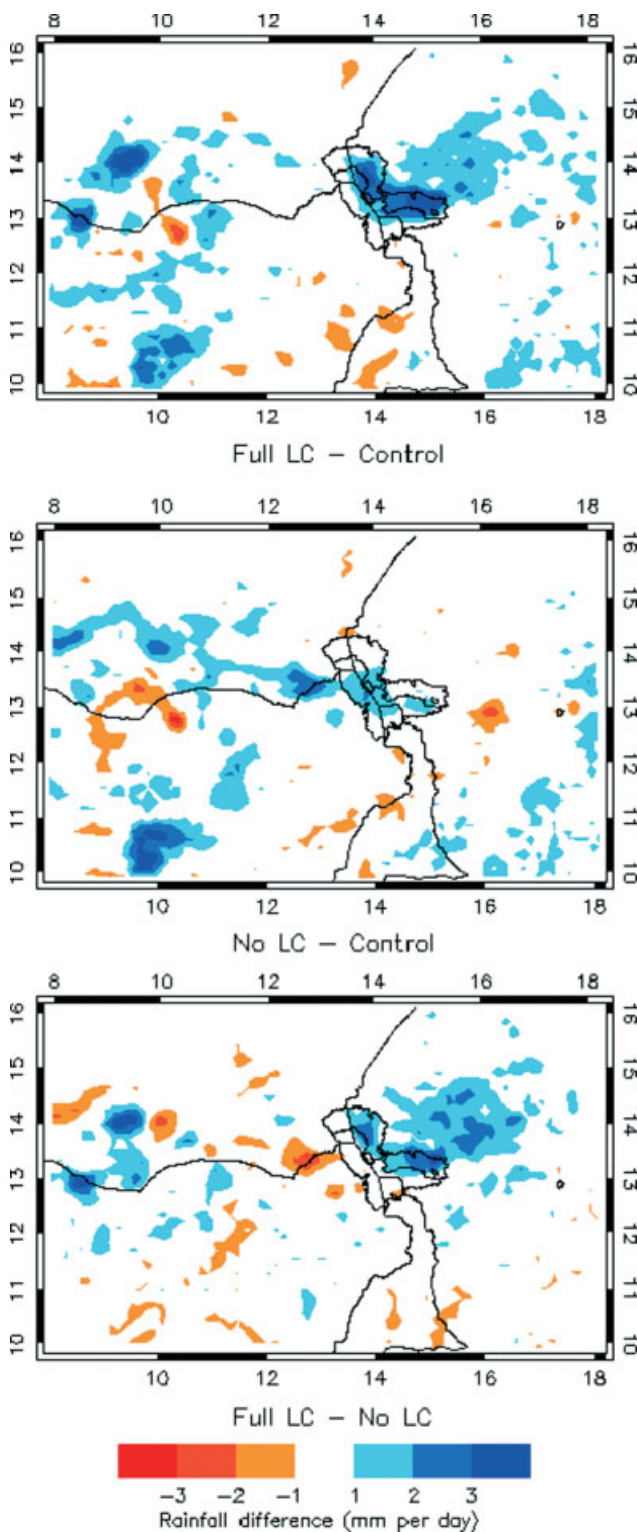
Figure 8. Rainfall difference maps for the entire simulated period (mm d^{-1}).

Table II. Moisture recycling ratio (%) for the total study area and the area where most precipitation changes occur.

	Control	Full LC	No LC
8−18°E; 10−16°N	6.35	7.09	6.28
12−17°E; 12.5−15°N	2.55	3.95	2.17

filled Lake Chad are thus likely to have a noticeable impact on passing mesoscale convective systems, which is investigated in section 4.4.

4.3. Hydrological cycle

When considering a large open water body such as Lake Chad in the semi-arid Sahel environment, it is interesting to know how significant the contribution of local evaporation is to the atmospheric moisture and hence the regional precipitation. Therefore the atmospheric components of the hydrological cycle are calculated for both the total study area and the area where the largest precipitation changes can be noticed (Table I). The balance of the atmospheric part of the water cycle (Peixoto and Oort, 1984) is

$$Q_{in} - Q_{out} = Rain - E + dQ_{dom}, \qquad (1)$$

where Q_{in} is the incoming atmospheric moisture, Q_{out} is the outgoing atmospheric moisture, Rain is the total rainfall in the area, E is the total evaporation in the area and dQ_{dom} is the change in atmospheric moisture content.

From Table I it is clear that the evaporation and rainfall in the area are small compared to the moisture fluxes – even hardly significant in the small domain. During the wet season in the Sahel, moist air is transported eastward by the AEJ (Figure 4(c)), which is located nearby the Lake Chad latitude for a large part of the simulated period, accounting for the largest part of the moisture flux. For the large domain, filling Lake Chad has a small positive effect on evaporation and rainfall amounts. The desiccation of the lake has almost no effect on the hydrological cycle for this area. In the surroundings of the lake, however, there is a significant increase in evaporation and rainfall when the lake is full. A small negative effect is visible when the remains of the lake would disappear.

In order to assess the importance of the evaporation from Lake Chad as a feedback to the atmospheric moisture, the moisture recycling ratio can be calculated. Schar *et al.* (1999) proposed a formula that can be used over large regions:

$$\beta = \frac{E}{E + Q_{in}} \qquad (2)$$

where β is the recycling ratio. Table II shows the results for the large and the small domain. The recycling ratios are very small during the simulated period and the effect of Lake Chad is not so large. It should be mentioned that this parameter is normally calculated for a whole year, which would increase its value as the moisture flux decreases and the evaporation from the lake increases during the dry season. Given this fact, the values for the Lake Chad environment are comparable to the moisture recycling values of 11% for the Nile and 8% for the Mississippi basins, reported by Mohamed *et al.* (2005). A notably larger value of 17% is found for the Amazon basin from the results of Eltahir and Bras (1994).

humidity was also limited to the lower atmosphere in the region of disturbance and downwind. These changes were found to have a negligible effect on the rainfall during the wet season. In the West African Sahel, however, anomalies of temperature and moisture in the boundary layer were found to have a significant impact on passing convective systems (Clark *et al.*, 2004). Taylor and Clark (2001) demonstrated that anomalies of 0.5 K and 0.5 g kg^{-1} can already modulate the characteristics of convection. The changes induced by a
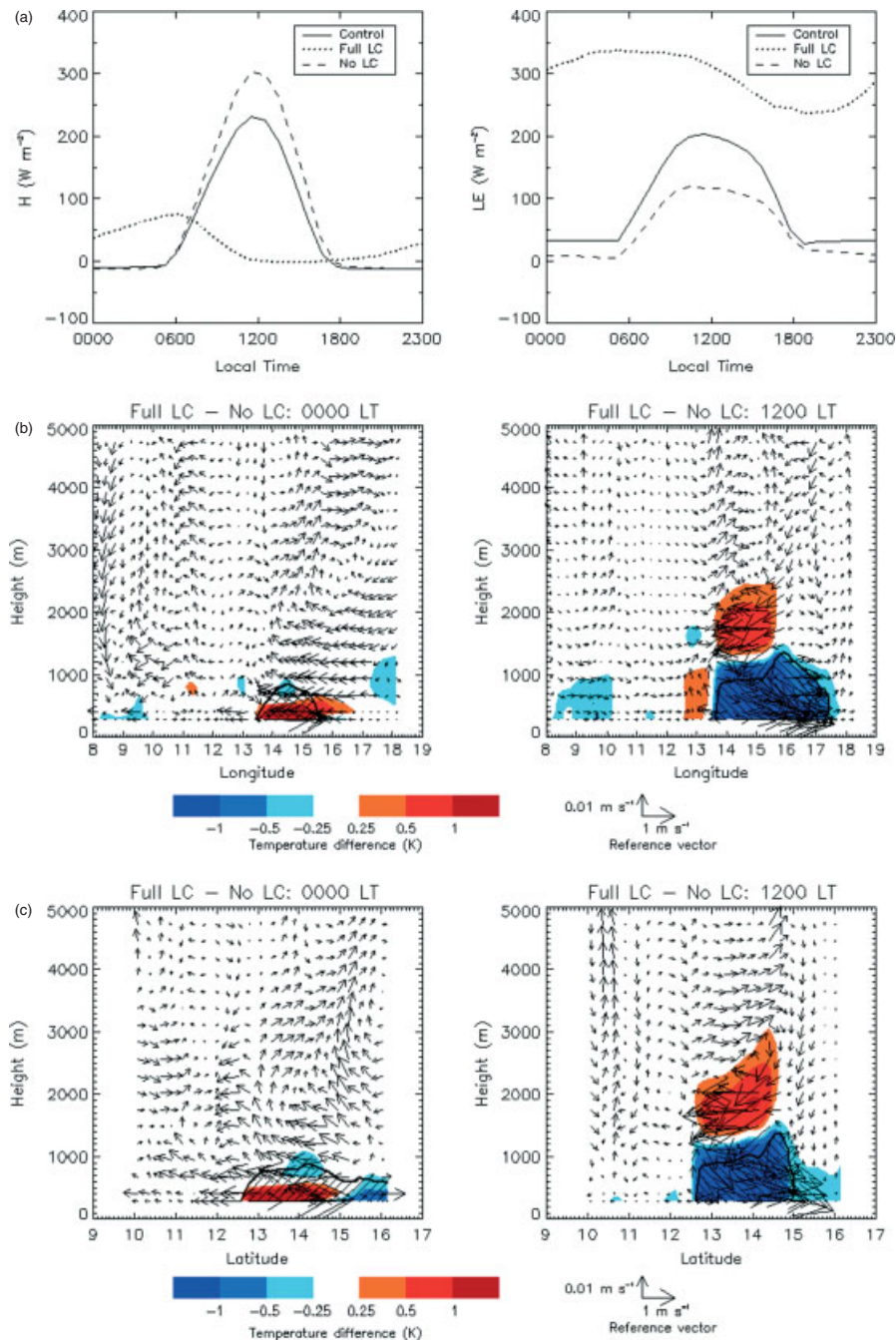
Figure 9. (a) Three-month mean values of sensible and latent heat fluxes over Lake Chad for the three scenarios. (b) Difference maps for 3-month mean values of temperature, specific humidity and wind speeds at 0000 and 1200 LT. Longitudinal cross-sections at 13.3°N. The hatched area with solid boundary defines the area where q increases by more than 1 g kg^{-1}. Note the different scaling for the horizontal and vertical wind components. (c) The same as b for latitudinal cross-sections at 14.5°E.

Based on these model results of the rainfall season in 2006, we can thus conclude that Lake Chad is not likely to have a strong effect on the regional hydrology during the wet season but it does have an effect on local components of the hydrological cycle.

4.4. Passing MCS

As mentioned in section 4.2, the effect of Lake Chad on the boundary layer temperature and humidity can be expected to have a noticeable influence on the development of convection in the region. To investigate this, a typical mesoscale convective system case is selected and compared for the scenario without a lake and the scenario with a

completely filled Lake Chad. The selected MCS passed the study area on 17 July 2006 in the model runs. There was no rainfall in the Lake Chad environment in the days prior to the arrival of the convective system, so the lake could influence the downwind boundary layer for a long time. In Figure 10(a), the cloud situation during the most intense phase of convection is displayed. When there is no lake, the convection develops into a typical westward-moving mesoscale convective system. When a large Lake Chad is present, on the other hand, the convection seems to be blocked by the lake and it does not progress over the lake. After a while, it dies out at the eastern side of the lake (not shown).
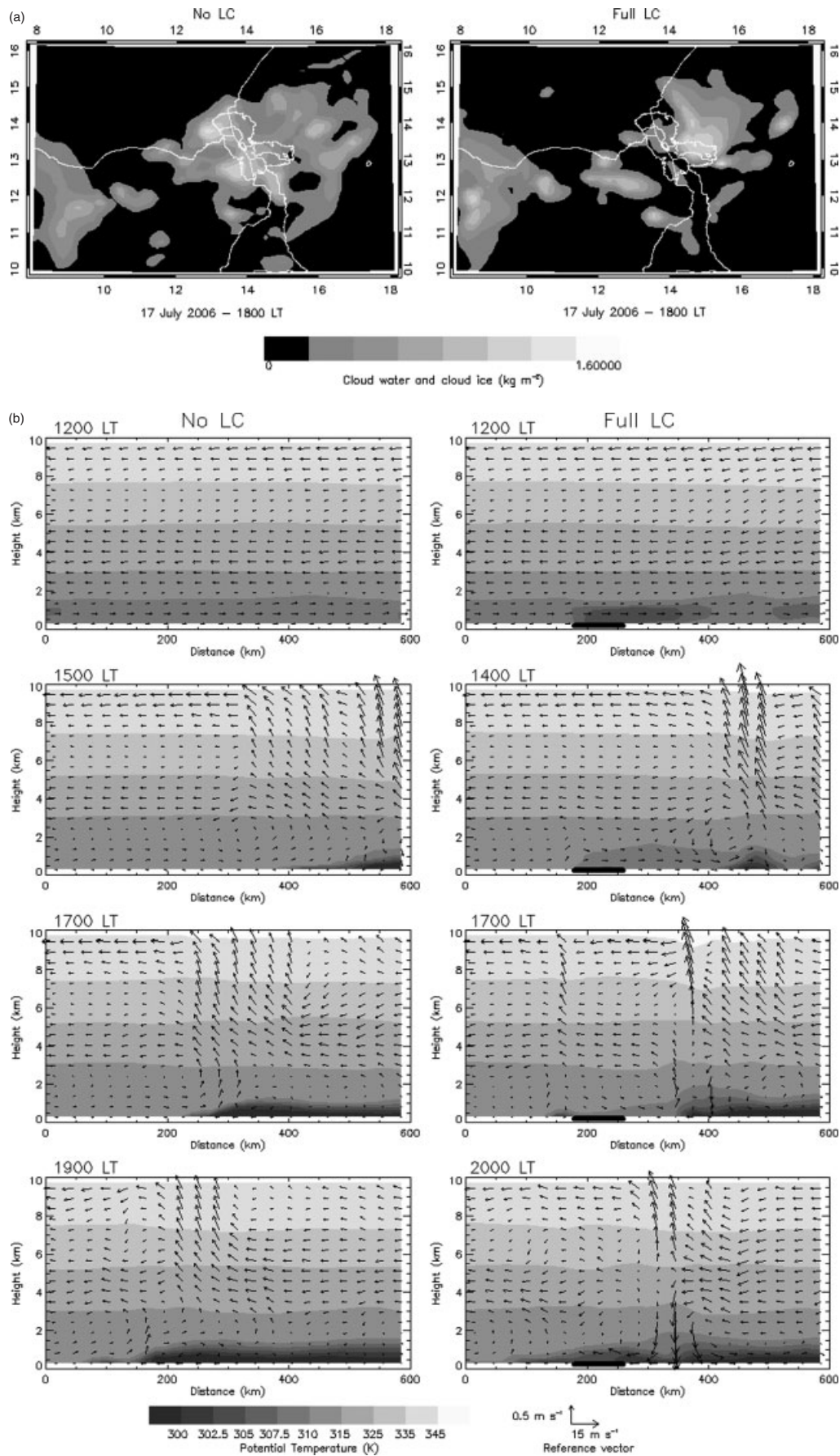
Figure 10. (a) Cloud situation for the MCS case occurring on 17 July 2006. (b) Vertical cross-sections of wind fields and potential temperatures along the transect 11.75°E, 13.5°N−17.5°E, 13.5°N. The location of Lake Chad is denoted by a black line. Note the different scaling for the horizontal and vertical wind components.

To understand the differences between both convective systems, vertical cross-sections along 13.5°N are shown in Figure 10(b). Statistics about the MCS passage are presented in Table III. For the No LC scenario, the thermodynamic structure of the atmosphere is horizontally homogeneous before the convection arrives. At the surface, winds blow from west to east, whereas the AEJ is present at 4 km height. When the convection arrives in the study area, it develops into a structured, fast westward-moving convective system. The thermodynamic structure of the fully developed convective system at the lower-left panel of Figure 10(b) compares very well with the observations of such an MCS in the Sahel, made by Chong *et al.* (1987).

Roux *et al.* (1984) describe the main characteristics of the circulation scheme of an MCS. The frontal updraft is maintained due to the collision of ambient air with the propagating cold pool. Important is the temperature difference between the environmental air and the colder frontward flow. The potentially unstable air in the front of the system is lifted up to an altitude around 3000 m, during which thermally driven convection may develop. Water loading and mixing with environmental colder air may reduce buoyancy, but once the water content is released through precipitation further convective updrafts up to 10 km height appear. The cold frontward flow over the surface results from the propagation of a cold air pool which is fed by evaporative downdrafts in the trailing stratiform region (visible between 400 and 600 km at 1900 LT in the lower-left panel of Figure 10(b)). The cold pool dynamics are found to be important for the propagation of MCS (Houze, 2004).

In case of a full Lake Chad, the situation is clearly different. Evaporation from the lake cools and moistens the overlying air which is transported eastwards by the surface winds, forming a plume of moist and cold air over a distance of several hundred kilometres. As this air is moister than in the No LC case, it has more CAPE, as can be seen in Table III. When the convective system arrives in the study area, the surplus in CAPE leads to stronger updrafts and higher precipitation amounts. However, the system is slower to advance as the cold pool encounters air that is almost as cool and moist. Table III shows that the difference in potential temperature of the cold pool and the air in front of the system is related to the MCS velocity. As mentioned before, the temperature difference between the cold frontal flow and the ambient air is important for the storm to develop a persistent internal circulation. The cold pool propagation is considerably less effective in lifting up the air in front of the storm as it approaches Lake Chad, leading to a weakening of the internal circulation and an inhibition of new convective cells within the MCS. The frontal updrafts slow down and completely disappear over Lake Chad, which can be seen on the lower right panel of Figure 10(b).

The mechanism discussed above could explain the higher rainfall amounts over the eastern side of Lake Chad and the lower amounts over the western side in the Full LC scenario (Figure 8). To test the hypothesis that the westward-moving convective systems become more intense on the east side of the lake, the number of times an updraft of more than 1 m s^{-1} is observed in a model grid point is counted for the total simulated period. At the resolution used in the model (15 km), such strong updrafts only exist in the most intense convective region of an MCS. Figure 11 shows the outcome of this analysis. The results confirm the hypothesis as there is

a large difference in the number of intense updrafts detected at the eastside of the lake during the 3-month simulations. When there is no lake, some intense systems are detected just west of the Lake Chad area, which is not the case when the lake is full.

To assess the influence of the lake temperature on this mechanism, two more scenario simulations with a full Lake Chad are performed, applying the minimum (300 K) and maximum (308 K) temperature values that are reported in the International Lake Environment Committee database. The statistics in Table III show that a warmer Lake Chad causes even higher CAPE values and more intense updrafts, with a slightly higher progression speed of MCS. A colder Lake Chad, on the other hand, results in a significantly less intense MCS with a slower progression speed, due to the colder air which is coming from the lake. Hence the lake temperature has a significant effect on the way the lake interacts with a passing MCS. Also, this interaction will be affected by the time of day an MCS passes, as the lake is warmer than the environment during the night and an MCS can be expected to progress faster through this warm air.

Related studies of the interaction of MCS with the environment are in line with our results with the Lake Chad experiments. Studying the passage of an MCS in the Sahel, Taylor *et al.* (1997) proposed a positive feedback between a moister boundary layer and rainfall intensity from a storm system, due to larger CAPE values. Clark *et al.* (2004) investigated the effect of different wet patches on subsequent rainfall in the Sahel by idealized model experiments. They also found a positive impact on rainfall intensities, with the strongest response at length scales of 10–15 km. Regarding convective initiation, on the other hand, the suppression of new convective systems and clouds over regions with very high latent heat fluxes is demonstrated in an observational study by Segal *et al.* (1998). Based on satellite observations, Taylor and Ellis (2006) also found wet patches to suppress convective initiation in the Sahel. In their mesoscale model experiments, Cheng and Cotton (2004) also showed that wetter soils suppress the initiation of convection in a semi-arid environment. We can thus conclude that a full Lake Chad enhances existing convective systems in its downwind area, whereas the further initiation of convective cells within an MCS is suppressed over the lake.

5. Conclusions

This paper has investigated the impact of the desiccation of Lake Chad on passing mesoscale convective systems and the local meteorology. The lake is located in the semi-arid Sahel area and shrunk from 25 000 km^2 to only 1350 km^2 over the last 50 years. Three scenarios were applied in our model experiments: Lake Chad as it was before the droughts, the current situation and a potential future scenario in which the lake and the surrounding wetlands are completely gone. The atmospheric model simulated the rainfall season of 2006 (July–September) for all three scenarios and was able to satisfactorily reproduce the overall structure of the rainfall amounts and atmospheric profiles.

It is an appealing idea that the massive water surface in this semi-arid area would lead to a large increase in rainfall over the Sahel if Lake Chad were to return to its old volume. Our results clearly showed that a widespread rainfall increase is unlikely. The further desiccation of the lake area had almost no effect on the simulated rainfall pattern. Also, the regional

Table III. Statistics of the MCS passage of 17 July 2006 in the area just east of Lake Chad ($15-16°$E, $13-14°$N).

	No LC	Full LC	Full LC warm	Full LC cold
θ (K)	310.2	306.6	306.3	304.8
$\theta_{\text{cold pool}}$ (K)	297.5	298.3	297.8	296.9
$\Delta\theta$ (K)	12.7	8.3	8.5	7.9
MCS vel. (m s^{-1})	16.9	15.9	16.1	15.0
CAPE (J kg^{-1})	2418	3174	3745	2257
Mean W_{max} (m s^{-1})	0.35	0.60	0.62	0.28

θ, potential temperature at 1200 LT; $\theta_{\text{cold pool}}$, potential temperature of the cold pool when it passed the area; $\Delta\theta$, difference between both potential temperatures; MCS vel., velocity of the MCS when it passed through the area: CAPE, convective available potential energy at 1200 LT; Mean W_{max}, area mean maximum vertical wind speed when the MCS passed through the area.
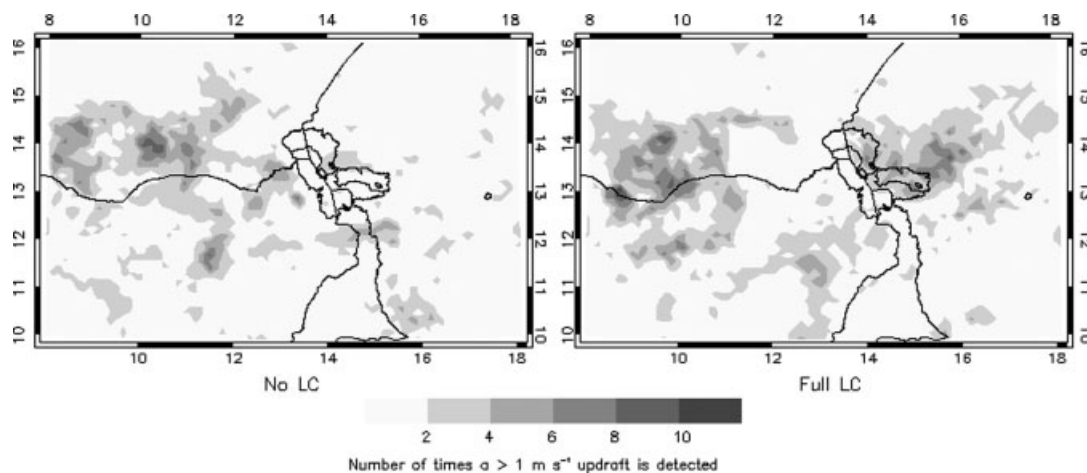

Figure 11. Surface maps of the number of times an updraft exceeding 1 m s^{-1} is detected in a certain grid point during the simulated period.

hydrological cycle was found to be hardly affected by the existence of the lake. These conclusions are consistent with related studies (e.g. Hope *et al.*, 2004; Segal *et al.*, 1998).

When investigating the impact of a large Lake Chad on the atmospheric environment, a significant cooling and moistening of the boundary layer downwind the lake was found. The magnitude of this effect could be expected to have a noticeable influence on the development of convection and the passing mesoscale convective systems. To assess this in detail, an MCS case was selected to investigate changes in the thermodynamic structure of the system. The effect of Lake Chad on the downwind boundary layer at first intensified the convection due to the large CAPE values of the moist air. However, the progression of the convective system was slowed down as the important cold pool propagation became less effective in the cold and moist air nearby Lake Chad. Further analysis revealed that this mechanism is affected by the lake temperature and the time of the day.

6. Appendix

6.1. Calculation of the Vegetation Cover and Leaf Area Index

The Satellite Pour l'Observation de la Terre (SPOT) 5 Vegetation monthly composite normalized difference vegetation index (NDVI) values are used to calculate the amount of vegetation cover in the month of July, using the relation

$$\text{Cover}_{\text{Jul}} = \frac{\text{NDVI} - \text{NDVI}_{\text{min}}}{\text{NDVI}_{\text{max}} - \text{NDVI}_{\text{min}}} \quad (3)$$

with NDVI$_{\text{min}}$ and NDVI$_{\text{max}}$ the minimum and maximum NDVI values in the domain region (Wittich and Hansing, 1995). The vegetation cover is assumed constant during each month of the simulated period.

To take into account the growing and wilting of the Sahelian vegetation during August and September, a new vegetation cover value per pixel is calculated for each month, based on the spatial relationship between the monthly NDVI images of July and August or September:

$$\text{Cover}_{\text{Aug}} = a_1 \cdot \text{Cover}_{\text{Jul}}^6 + a_2 \cdot \text{Cover}_{\text{Jul}}^5 + a_3 \cdot \text{Cover}_{\text{Jul}}^4$$
$$+ a_4 \cdot \text{Cover}_{\text{Jul}}^3 + a_5 \cdot \text{Cover}_{\text{Jul}}^2 + a_6 \cdot \text{Cover}_{\text{Jul}} + a_7 \quad (4)$$
$$\text{Cover}_{\text{Sep}} = b_1 \cdot \text{Cover}_{\text{Jul}}^6 + b_2 \cdot \text{Cover}_{\text{Jul}}^5 + b_3 \cdot \text{Cover}_{\text{Jul}}^4$$
$$+ b_4 \cdot \text{Cover}_{\text{Jul}}^3 + b_5 \cdot \text{Cover}_{\text{Jul}}^2 + b_6 \cdot \text{Cover}_{\text{Jul}} + b_7 \quad (5)$$

where Cover$_{\text{Jul}}$ is the vegetation cover value of a model grid point in July 2006 and a_n and b_n are constants. Note that the vegetation cover values in the desert (<0.05) and in densely vegetated areas (>0.75) are kept constant, as the comparison of the NDVI images shows no growing or wilting in these regions.

Leaf area index (LAI) values are obtained from the spatial relationship between monthly mean MODerate-resolution Imaging Spectroradiometer (MODIS) LAI values of Augustus 2006 and the vegetation cover values of the same month. This relationship is empirically derived for the model domain, using the relation

$$\text{LAI} = d_1 \cdot \text{Cover}^6 + d_2 \cdot \text{Cover}^5 + d_3 \cdot \text{Cover}^4$$
$$+ d_4 \cdot \text{Cover}^3 + d_5 \cdot \text{Cover}^2 + d_6 \cdot \text{Cover} \quad (6)$$

where Cover is the vegetation cover value of a model grid point and d_n are constants. This leads to maximum LAI values in the model domain of 4.5. Note that when the vegetation cover changes from one month to the other, also the LAI values change slightly, as the same relationship is used during all simulated months. This can be done because the relationship between vegetation cover and LAI values is not found to change over time during the modelled period.

Acknowledgements

References

Agusti-Panareda A, Beljaars A, Cardinali C, Genkova I, Thorncroft C. 2010. Impacts of assimilating AMMA soundings on ECMWF analyses and forecasts. *Weather and Forecasting* 25(4): 1142−1160.

Agusti-Panareda A, Vasiljevic D, Beljaars A, Bock O, Guichard F, Nuret M, Garcia Mendez A, Andersson E, Bechtold P, Fink A, Hersbach H, Lafore J-P, Ngamini J-B, Parker DJ, Redelsperger J-L, Tompkins AM. 2009. Radiosonde humidity bias correction over the West African region for the special AMMA reanalysis at ECMWF. *Q. J. R. Meteorol. Soc.* 135: 595−617.

Andersson E, Bauer P, Beljaars A, Chevallier F, Holm E, Janiskova M, Kallberg P, Kelly G, Lopez P, McNally A, Moreau E, Simmons J, Thepaut JN, Tompkins AM. 2005. Assimilation and modeling of the atmospheric hydrological cycle in the ECMWF forecasting system. *Bull. Am. Meteorol. Soc.* 86: 387−402.

Birkett CM. 2000. Synergistic remote sensing of Lake Chad: variability of basin inundation. *Remote Sens. Environ.* 72: 218−236.

Bonan GB. 1995. Sensitivity of a GCM simulation to inclusion of inland water surfaces. *J. Climate* 8: 2691−2704.

Cheng WYY, Cotton WR. 2004. Sensitivity of a cloud-resolving simulation of the genesis of a mesoscale convective system to horizontal heterogeneities in soil moisture initialization. *J. Hydrometeorol.* 5: 934−958.

Chong M, Amayenc P, Scialom G, Testud J. 1987. A tropical squall line observed during the Copt-81 experiment in West Africa. 1. Kinematic structure inferred from dual-Doppler radar data. *Mon. Weather Rev.* 115: 670−694.

Clark DB, Taylor CM, Thorpe AJ. 2004. Feedback between the land surface and rainfall at convective length scales. *J. Hydrometeorol.* 5: 625−639.

De Ridder K, Schayes G. 1997. The IAGL land surface model. *J. Appl. Meteorol.* 36: 167−182.

Eltahir EAB, Bras RL. 1994. Precipitation recycling in the Amazon basin. *Q. J. R. Meteorol. Soc.* 120: 861−880.

Goyens C, Lauwaet D, Schröder M, Demuzere M, van Lipzig NPM. 2011. Tracking mesoscale convective systems in the Sahel: relation between cloud parameters and precipitation. *International Journal of Climatology* (in press).

Hope PK, Nicholls N, McGregor JL. 2004. The rainfall response to permanent inland water in Australia. *Aust. Meteorol. Mag.* 53: 251−262.

Houze RA. 2004. Mesoscale convective systems. *Rev. Geophys.* 42: RG4003, DOI:10.1029/2004RG000150.

Hutchinson CF, Warshall P, Arnould EJ, Kindler J. 1992. Development in arid lands: lessons from Lake Chad. *Environment* 34: 16−20.

Kain JS, Fritsch JM. 1990. A one-dimensional entraining detraining plume model and its application in convective parameterization. *Journal of the Atmospheric Sciences* 47: 2784−2802.

Laurent H, D'Amato N, Lebel T. 1998. How important is the contribution of the mesoscale convective complexes to the Sahelian rainfall? *Phys. Chem. Earth* 23: 629−633.

Lauwaet D, De Ridder K, van Lipzig NPM. 2008. The influence of soil and vegetation parameters on atmospheric variables relevant for convection in the Sahel. *J. Hydrometeorol.* 9: 461−476.

Lauwaet D, van Lipzig NPM, De Ridder K. 2009. The effect of vegetation changes on precipitation and mesoscale convective systems in the Sahel. *Clim. Dynam.* 33: 521−534.

Mathon V, Laurent H, Lebel T. 2002. Mesoscale convective system rainfall in the Sahel. *J. Appl. Meteorol.* 41: 1081−1092.

Mohamed YA, van den Hurk B, Savenije HHG, Bastiaanssen WGM. 2005. Impact of the Sudd wetland on the Nile hydroclimatology. *Water Resour. Res.* 41: W08420, DOI: 10.1029/2004WR003792.

Mohr KI, Baker RD, Tao WK, Famiglietti JS. 2003. The sensitivity of West African convective line water budgets to land cover. *J. Hydrometeorol.* 4: 62−76.

Peixoto JP, Oort AH. 1984. Physics of climate. *Rev. Modern Phys.* 56: 365−429.

Roux F, Testud J, Payen M, Pinty B. 1984. West-African squall-line thermodynamic structure retrieved from dual-Doppler radar observations. *J. Atmos. Sci.* 41: 3104−3121.

Schar C, Luthi D, Beyerle U, Heise E. 1999. The soil-precipitation feedback: a process study with a regional climate model. *J. Climate* 12: 722−741.

Schröder M, Köning M, Schmetz J. 2009. Deep convection observed by the spinning enhanced visible and infrared imager on board Meteosat8: spatial distribution and temporal evolution over Africa in summer and winter 2006. *J. Geophys. Res.* 114: D05109, DOI: 10.1029/2008JD010653.

Schultz P. 1995. An explicit cloud physics parameterization for operational numerical weather prediction. *Mon. Weather Rev.* 123: 3331−3343.

Segal M, Leuthold M, Arritt RW, Anderson C, Shen J. 1997. Small lake daytime breezes: some observations and conceptual evaluations. *Bull. Am. Meteorol. Soc.* 78: 1135−1147.

Segal M, Pan Z, Turner RW, Takle ES. 1998. On the potential impact of irrigated areas in North America on summer rainfall caused by large-scale systems. *J. Appl. Meteorol.* 37: 325−331.

Taylor CM, Clark DB. 2001. The diurnal cycle and African easterly waves: a land surface perspective. *Q. J. R. Meteorol. Soc.* 127: 845−867.

Taylor CM, Ellis RJ. 2006. Satellite detection of soil moisture impacts on convection at the mesoscale. *Geophys. Res. Lett.* 33: L03404, DOI: 10.1029/2005GL025252.

Taylor CM, Said F, Lebel T. 1997. Interactions between the land surface and mesoscale rainfall variability during HAPEX-Sahel. *Mont. Weather Rev.* 125: 2211−2227.

Taylor CM, Harris PP, Parker DJ. 2010. Impact of soil moisture on the development of a Sahelian mesoscale convective system: a case-study from the AMMA Special Observing Period. *Q. J. R. Meteorol. Soc.* 136: 456−470.

Vandervaere JP, Peugeot C, Vauclin M, Jaramillo RA, Lebel T. 1997. Estimating hydraulic conductivity of crusted soils using disc infiltrometers and minitensiometers. *J. Hydrol.* 189: 203−223.

Weaver CP. 2004. Coupling between large-scale atmospheric processes and mesoscale land-atmosphere interactions in the U.S. Southern Great Plains during summer. Part 1: Case studies. *J. Hydrometeorol.* 5: 1223−1246.

Wittich KP, Hansing O. 1995. Area-averaged vegetative cover fraction estimated from satellite data. *Int. J. Biometeorol.* 38: 209−215.

Xue M, Droegemeier KK, Wong V. 2000. The Advanced Regional Prediction System (ARPS): a multi-scale nonhydrostatic atmospheric simulation and prediction model. Part I: Model dynamics and verification. *Meteorol. Atmos. Phys.* 75: 161−193.

Xue M, Droegemeier KK, Wong V, Shapiro A, Brewster K, Carr F, Weber D, Liu Y, Wang D. 2001. The Advanced Regional Prediction System (ARPS): a multi-scale nonhydrostatic atmospheric simulation and prediction tool. Part II: Model physics and applications. *Meteorol. Atmos. Phys.* 76: 143−165.